

SUPERCONDUCTIVITY WS 15-16

Monday 10:00-11:30

SR Exp. physics II

Prof. Paul H.M. van Loosdrecht

pvl@ph2.uni-koeln.de

www.loosdrecht.net

Materials

- Elemental
- Intermetallics (Alloys, A15 & other Xtals)
- Fullerene based
- Organic superconductors
- Heavy fermion compounds
- Cuprates & oxides

Triplet superconductivity ?

VOLUME 88, NUMBER 1

PHYSICAL REVIEW LETTERS

7 JANUARY 2002

Triplet Superconductivity in an Organic Superconductor Probed by NMR Knight Shift

I. J. Lee,^{1,*} S. E. Brown,² W. G. Clark,² M. J. Strouse,³ M. J. Naughton,⁴ W. Kang,⁵ and P. M. Chaikin¹

Knight shift: Shift of resonance frequency in NMR due to spin coupling of nuclei to conduction electrons

$$K = \alpha \chi_{spin}$$

Singlet superconductor:

$K = 0$, change at $T_c \sim$ pauli susceptibility

Triplet superconductor:

no change at T_c

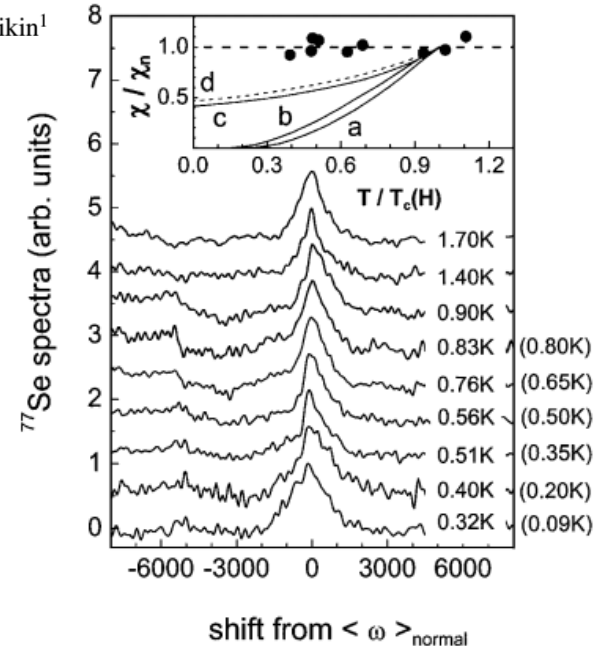
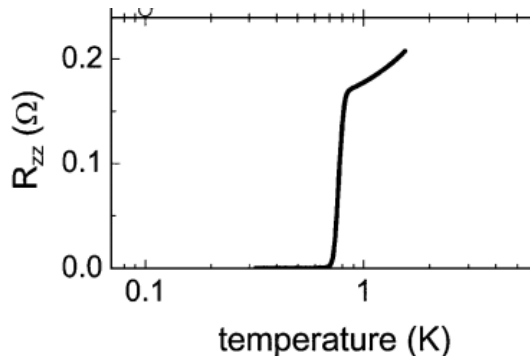


FIG. 3. ^{77}Se NMR spectra collected above and below T_c (0.81 K at 1.43 T). Each trace is normalized and offset for clarity. The temperatures shown in parentheses are the measured equilibrium temperatures before the pulse. In the inset, the spin susceptibility normalized by the normal state χ/χ_n from measured first moments are compared with Fulde and Maki's calculation for $H/H_{c2}(0) \sim 0$ (curve a) and 0.63 (curve b). Curves c and d are obtained from the ratio of applied field (1.43 T) to the measured upper critical field $H_{c2}(T)$ at which the superconducting criteria "onset" and "50% transition" have been used, respectively, to determine $H_{c2}(T)$.

Triplet superconductivity

- Cooper pair: bound state of 2 electrons
 - Singlet $|\uparrow\downarrow - \downarrow\uparrow\rangle/\sqrt{2}$
Triplet $|\uparrow\uparrow\rangle, |\downarrow\downarrow\rangle, |\uparrow\downarrow + \downarrow\uparrow\rangle/\sqrt{2}$
- Total wavefunction anti-symmetric under exchange electrons
 - Singlet \otimes even orbital wavefunction
L=0 (s-wave), 2 (d-wave), ...
 - Triplet \otimes odd orbital wavefunction
L=1 (p-wave), 3 (f-wave), ...

Real space wave functions (s,p,d superconductivity)

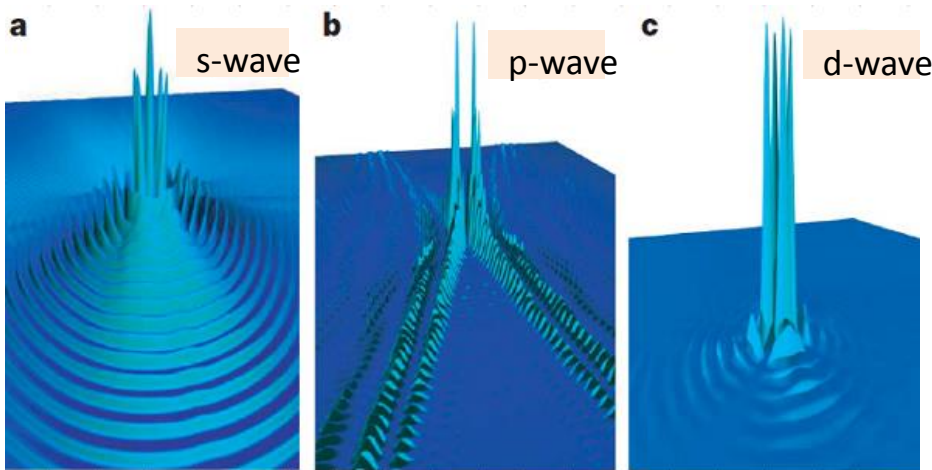


Figure 1 | Cooper-pair states in real space in two dimensions. a–c, The probability of finding one quasiparticle in a Cooper-pair state given that the other partner is at the origin. The symmetric form in **a** is characteristic of an s-wave spin-singlet state. The two-fold symmetry in **b** is characteristic of one of the possible *p*-wave spin-triplet states, whereas the four-fold symmetry in **c** is characteristic of a *d*-wave spin-singlet state. The Cooper-pair states

P. Monthoux, D. Pines & G. G. Lonzarich,
Review “Superconductivity without phonons” Nature 450, 1177 (2007)

s-wave:

$$\psi(0) \neq 0$$

Suppressed by on-site coulomb
Large spatial extend → weakly bound

d-wave

$$\psi(0) = 0$$

Avoids on-site coulomb
Large amplitude nearest neighbors
→ strong binding → high T_c

d-wave nature cuprates

FIG. 13. Three-dimensional rendering of a scanning SQUID microscope image of a thin-film YBCO tricrystal ring sample, cooled and imaged in nominally zero magnetic field. The outer control rings have no flux in them; the central three-junction ring has half of a superconducting quantum of flux spontaneously generated in it [Color].

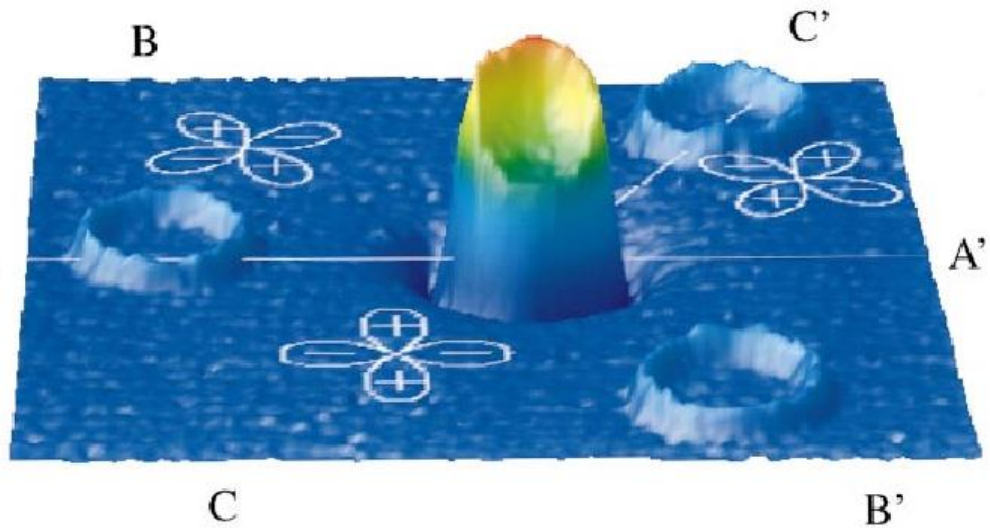
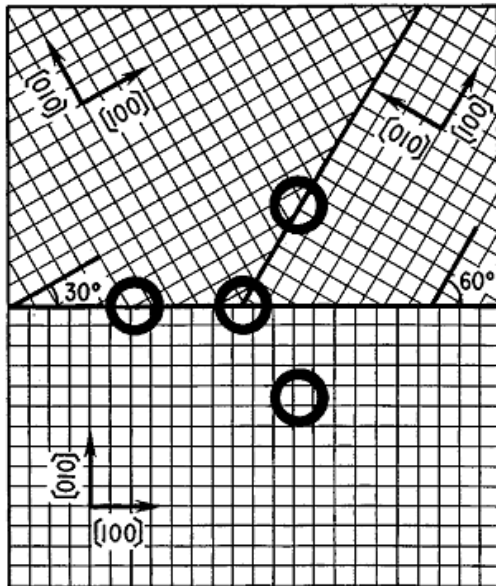
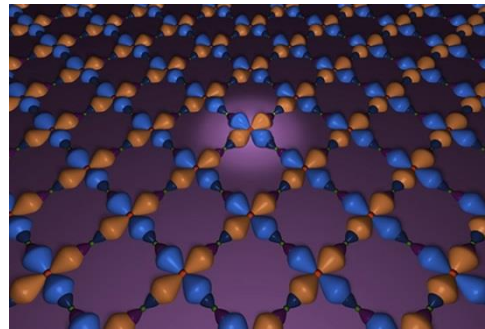
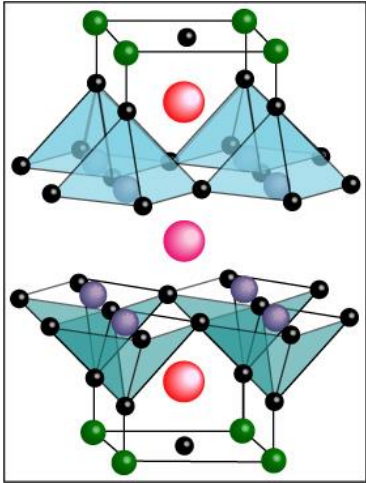


FIG. 11. Experimental configuration for the π -ring tricrystal experiment of Tsuei *et al.* (1994). The central, three-junction ring is a π ring, which should show half-integer flux quantization for a $d_{x^2-y^2}$ superconductor, and the two-junction rings and zero-junction ring are zero rings, which should show integer flux quantization, independent of the pairing symmetry.

Gap anisotropy, d-wave



Group-theoretic notation	A_{1g}	A_{2g}	B_{1g}	B_{2g}
Order parameter basis function	constant	$xy(x^2-y^2)$	x^2-y^2	xy
Wave function name	s-wave	g	$d_{x^2-y^2}$	d_{xy}
Schematic representation of $\Delta(k)$ in B.Z.				

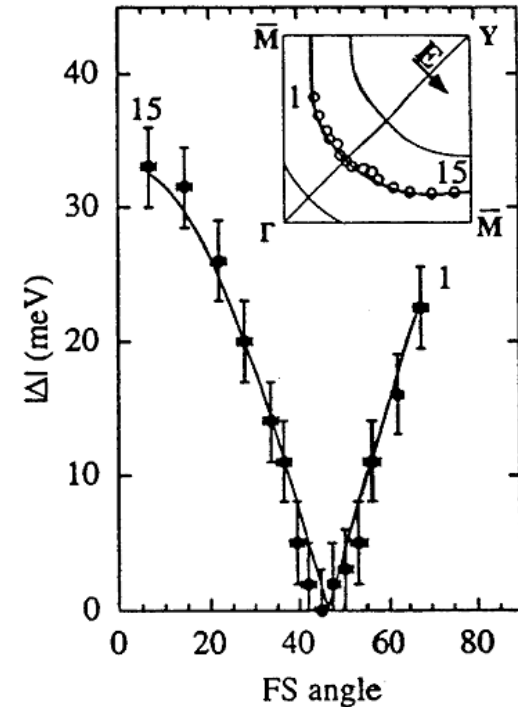
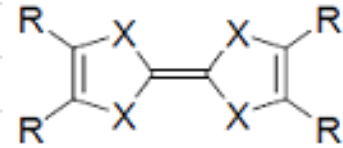


FIG. 4. Energy gap in Bi-2212: ●, measured with ARPES as a function of angle on the Fermi surface; solid curve, with fits to the data using a d -wave order parameter. Inset indicates the locations of the data points in the Brillouin zone. From Ding, Norman, *et al.* (1996).

Organic superconductors

Bechaard salts (D. Jérôme, A. Mazaud, M. Ribault et K. Bechgaard, J. Physique Lett. 41, 95-98 (1980))

- Charge transfer salts
 - Cation (donor) TMTSF (tetramethyltetraseleniafulvalene)
 - Anion (acceptor) PF_6 , ClO_4 , AsF_6 ,
- Quasi one-dimensional



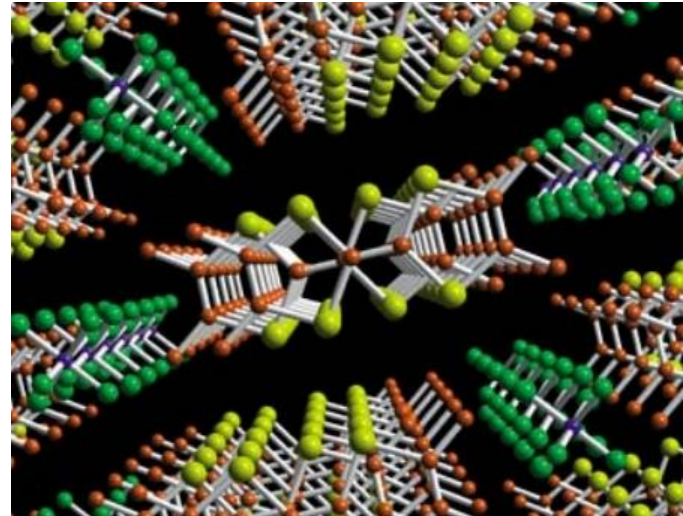
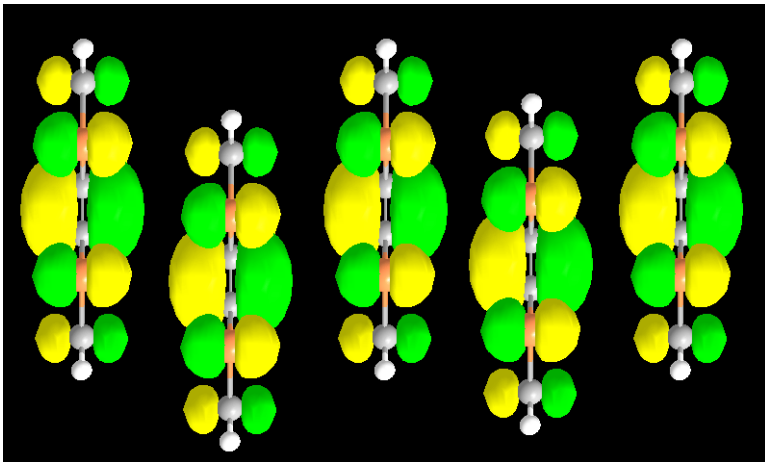
TTF : X=S, R=H

TSF : X=Se, R=H

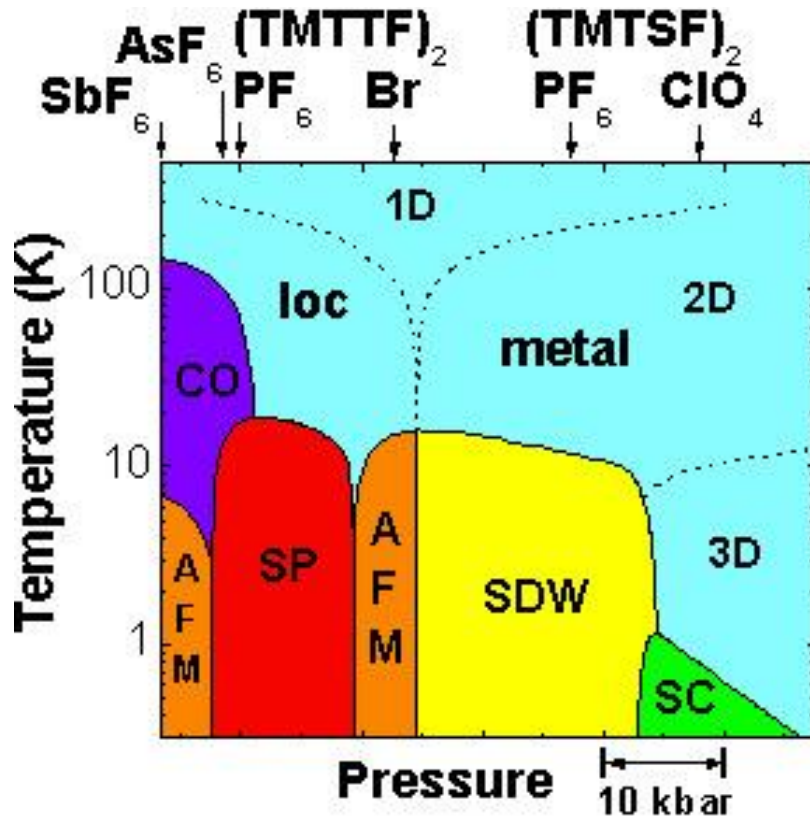
TTeF : X=Te, R=H

TMTSF : X=Se, R=Me

TMTTF : X=S, R=Me



Organic superconductors



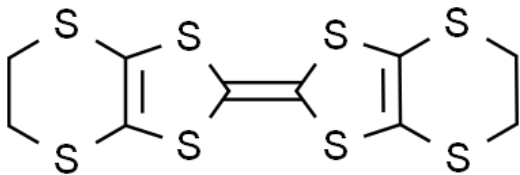
Material	TC (K)	pext (kbar)
(TMTSF) ₂ ClO ₄	1.4	0
(TMTSF) ₂ SbF ₆	0.36	10.5
(TMTSF) ₂ PF ₄	1.1	6.5
(TMTSF) ₂ AsF ₆	1.1	9.5
(TMTSF) ₂ ReO ₄	1.2	9.5
(TMTSF) ₂ TaF ₆	1.35	11
(TMTTF) ₂ Br	0.8	26

Complex electronic phase diagram
 Pressure enhances dimensionality
 when $t_{\text{perp}} \gg kT$

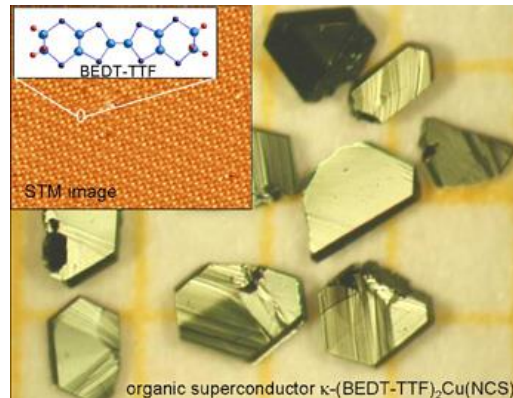
Organic superconductors

BEDT-TTF Salts (ET-salts)

- Charge transfer salts
Donor BEDT-TTF
Acceptor I_3 , $KHg(SCN)_4$, ...
- Two dimensional
Many different patterns: β , κ , θ , ...
- Possibly d-wave pairing



bisethylenedithio-
tetrathiafulvalene



Material	T_c (K)	p_{ext} (kbar)
β_H -(ET) $_2$ I $_3$	1.5	0
θ -(ET) $_2$ I $_3$	3.6	0
κ -(ET) $_2$ I $_3$	3.6	0
α -(ET) $_2$ KHg(SCN) $_4$	0.3	0
α' -(ET) $_2$ KHg(SCN) $_4$	1.2	1.2
β'' -(ET) $_2$ SF $_5$ CH $_2$ CF $_2$ SO $_3$	5.3	0
κ -(ET) $_2$ Cu[N(CN) $_2$]Cl	12.8	0.3
κ -(ET) $_2$ Cu[N(CN) $_2$]Cl deuterated	13.1	0.3
κ -(ET) $_2$ Cu[N(CN) $_2$]Br deuterated	11.2	0
κ -(ET) $_2$ Cu(NCS) $_2$	10.4	0
κ -(ET) $_4$ Hg $_{2.89}$ Cl $_8$	1.8	12
κ_H -(ET) $_2$ Cu(CF $_3$) $_4$ ·TCE	9.2	0
κ_H -(ET) $_2$ Ag(CF $_3$) $_4$ ·TCE	11.1	0

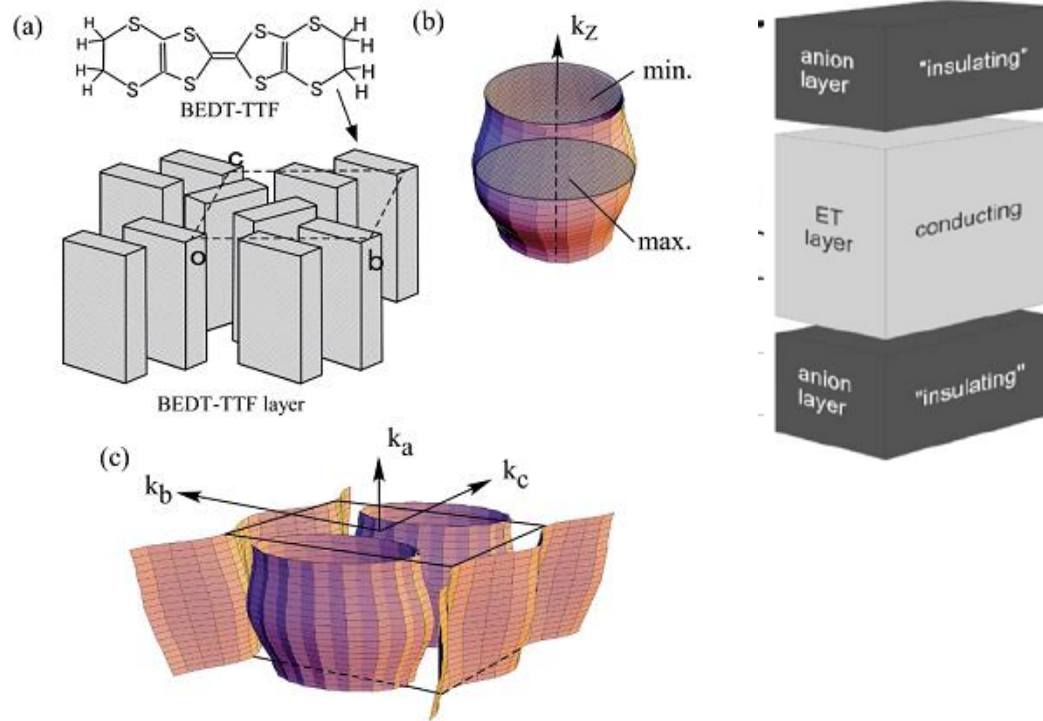
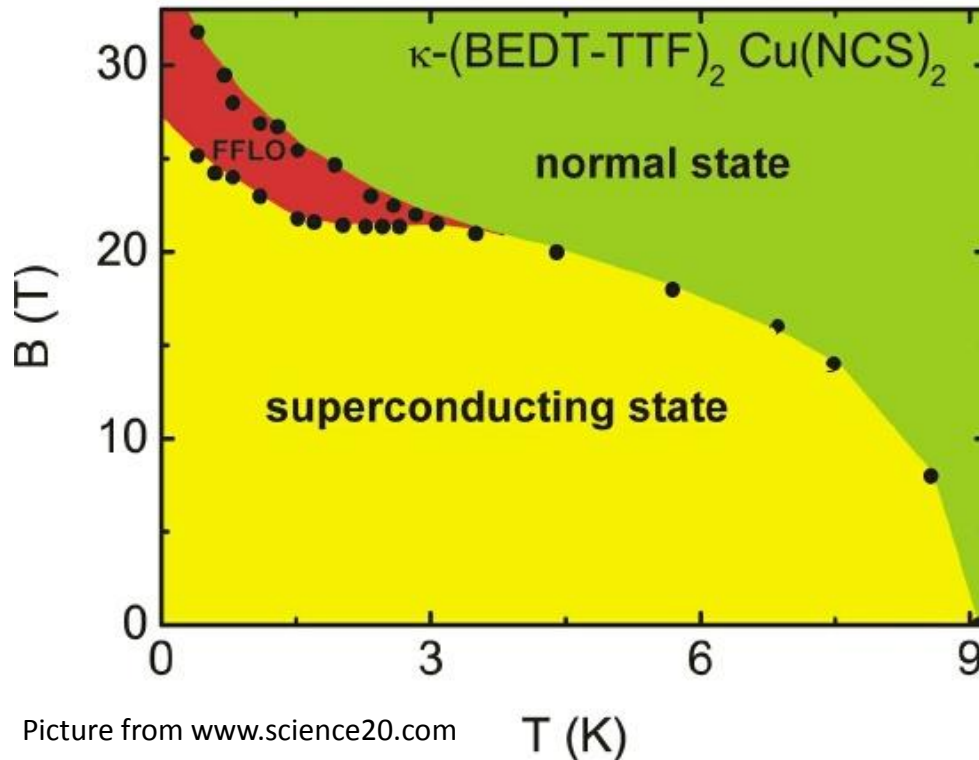


Fig. 6.1. (a) BEDT-TTF (ET) molecule and the ET packing arrangement (conducting layer) of an organic superconductor κ -(BEDT-TTF) $_2$ Cu(NCS) $_2$. The ET molecule (conducting) and Cu(NCS) $_2$ anion (insulating) layers stack alternately along the a axis. (b) A quasi-two-dimensional Fermi surface. When the field is applied along the cylindrical (k_z) axis, two extremal (minimum and maximum) cross sections are well defined, indicated by shaded areas. (c) The calculated Fermi surface of κ -(BEDT-TTF) $_2$ Cu(NCS) $_2$. The solid lines show the first Brillouin zone boundaries. There exist two open sheets of 1D Fermi surface and a closed 2D Fermi surface



Calorimetric Evidence for a Fulde-Ferrel-Larkin-Ovchinnikov Superconducting State in the Layered Organic Superconductor κ -(BEDT-TTF)₂Cu(NCS)₂

R. Lortz,¹ Y. Wang,² A. Demuer,² P. H. M. Böttger,³ B. Bergk,³ G. Zwicknagl,⁴ Y. Nakazawa,⁵ and J. Wosnitza³



Picture from www.science20.com

Normally SC state stable until
zeeman E can break pairs
Competing phase: SC formed from
spin-split normal state
→ FFLO state

- Finite q cooper pairs
- Spatially modulated order parameter

Heavy fermion systems

Heavy fermion materials

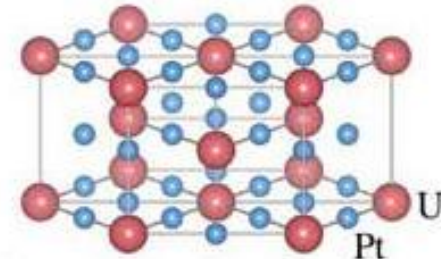
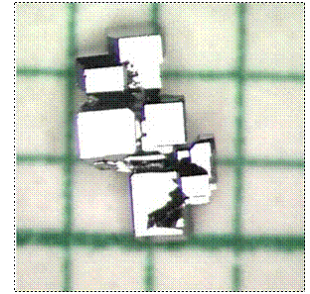
- partially filled f-shell compounds
- Strong on-site repulsion favoring localized spins
- hybridization with conduction electrons
- narrow bandwidth peak near Fermi level
- high effective mass
- Kondo physics

At high T:

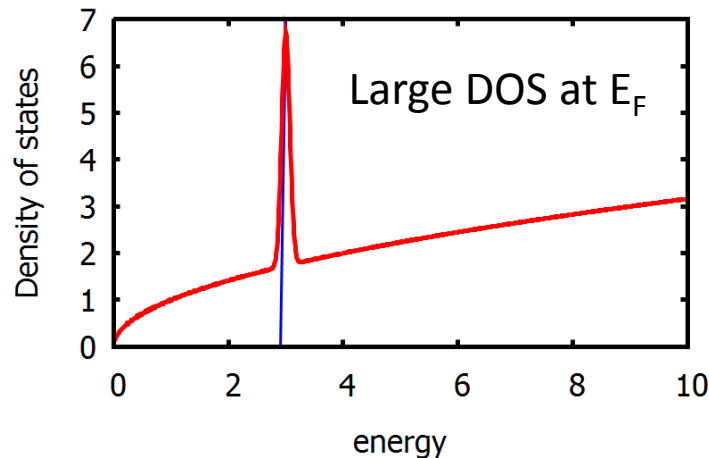
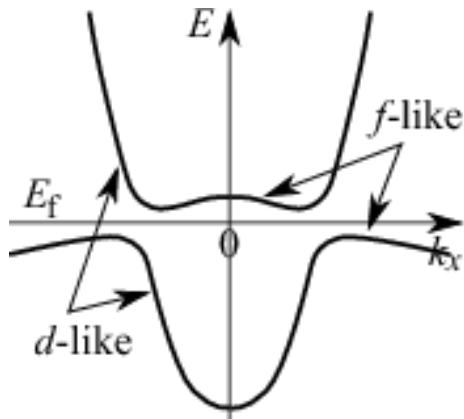
conduction electrons scatter on local spins

At low T ($\ll 10\text{K}$):

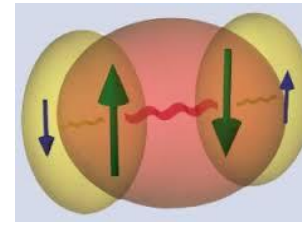
local spins screened by conduction electron spins



UPt₃



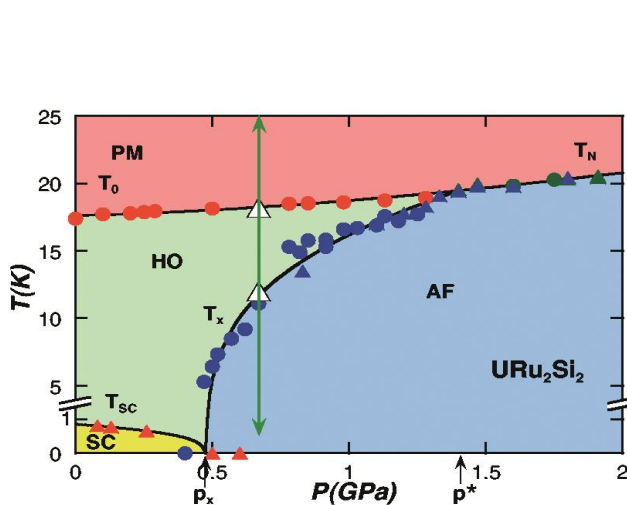
- High temperature phase often non-fermi liquid
 $\rho \sim T$ instead of T^2 (FL)
- Competition (& coexistence?) of SC and magnetism
- Strong on-site correlations not in favor of s-wave pairing
- Pairing of electronic origin?
- UPt_3 (and others) triplet superconductor
- Often SC in vicinity quantum critical point
- Record $T_c = 18.5$ K for $PuCoGa_5$ (Sarrao et al., Nature 2002)



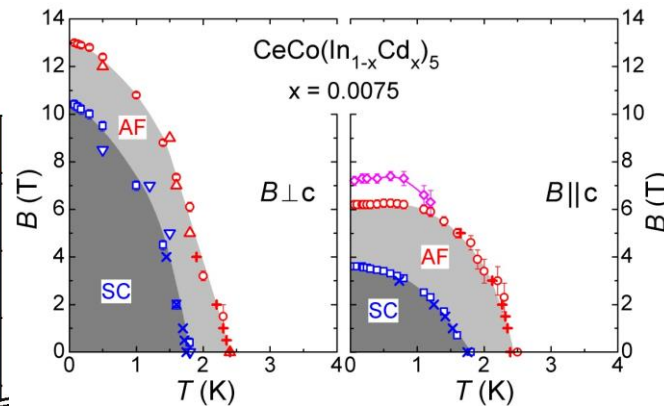
Electronic (Magnon) glue?

Material	T_c (K)
CeCu ₂ Si ₂	0.7
CeCoIn₅	2.3
CeIn ₃	0.2
UPt ₃	0.48
URu ₂ Si ₂	1.3
UPd ₂ Al ₃	2.0
UNi ₂ Al ₃	1.1

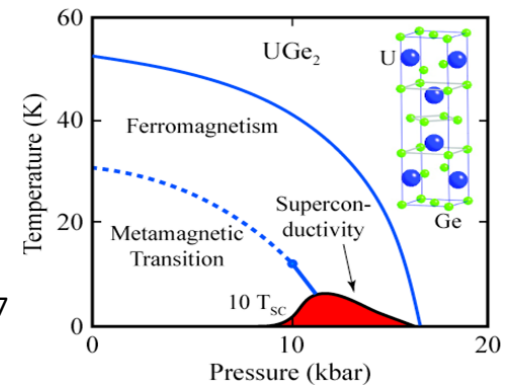
wikipedia



A. Villaume, et al., Physical Review B 78 (2008) 012504

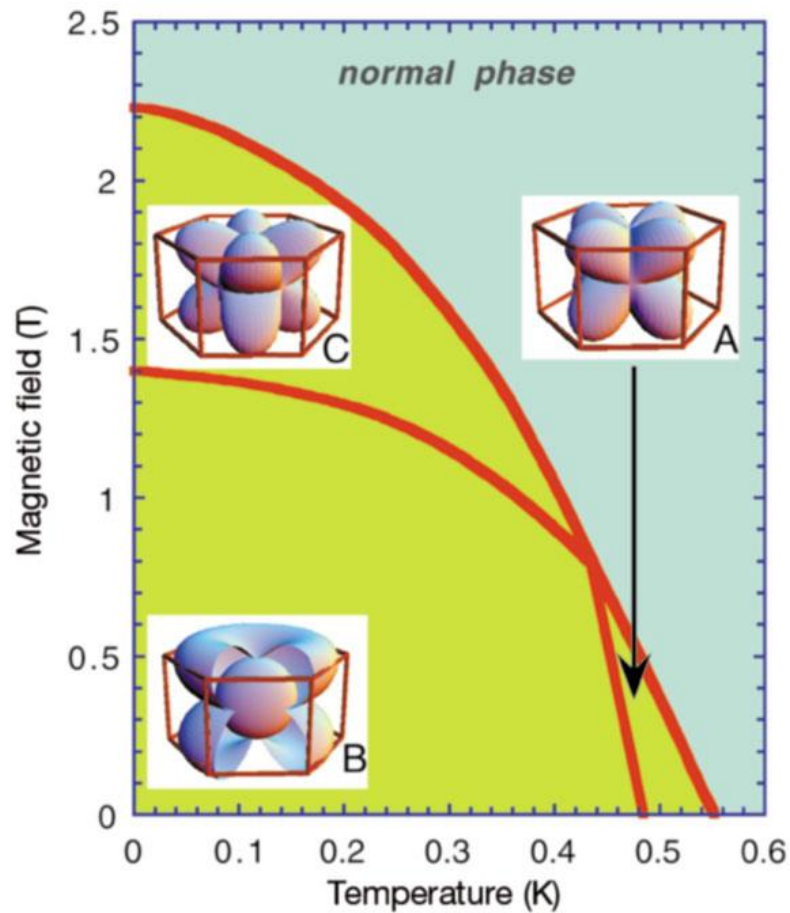


Sunil Nair et al., Proc. Natl. Acad. Sci. USA **107** (2010) 9537



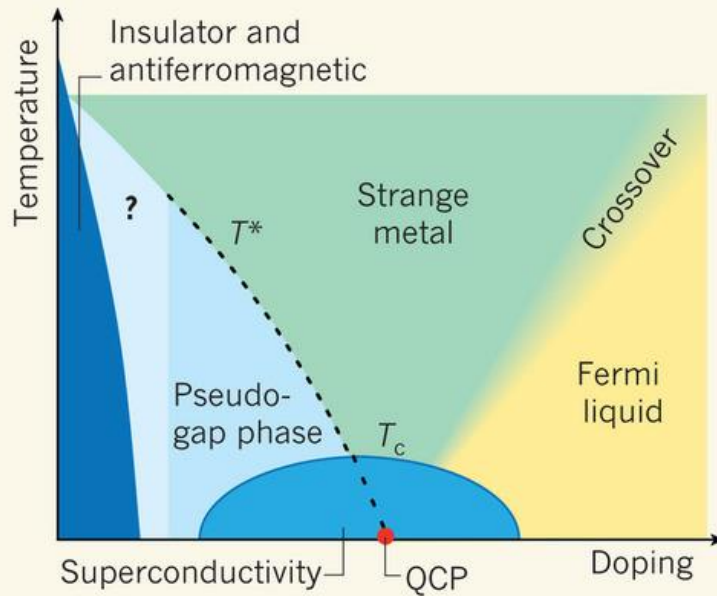
Dept. Physics, cambridge univ.

3 superconducting phases in UPt_3 (3 different gap symmetries)
derived from flux-lattice symmetry



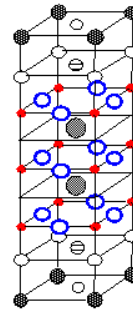
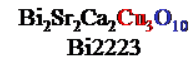
Huxley et al., Nature 406, 160 (2000)

Cuprates & other oxides

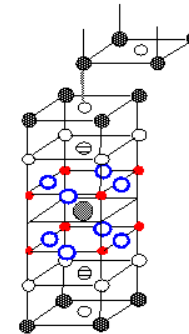
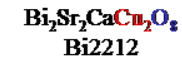


Chandra Varma, Nature 468, 184 (2010)

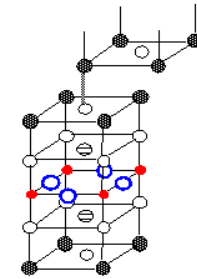
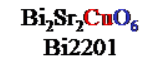
CuO planes are the key components of high T_c superconductors



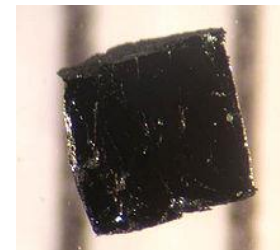
(3 CuO L)
 $T_c = 105 \text{ K}$



(2 CuO L)
 $T_c = 92 \text{ K}$



(1 CuO L)
 $T_c = 0 \sim 20 \text{ K}$



Bi2223, wikipedia

High Tc cuprates

Bednorz & Mueller, Z.Physik B 64, 189 (1986):

Ba-La-Cu-O ~30 K

Current record:

135 K in Hg-1223 (Chu et al, Nature 1993)

166 K in Hg-1223 (fluorinated)

@ 23 Gpa (Monteverde, EPL 2005)

2D planes → low dimensionality

Strong electron correlations (Mott-Hubbard physics)

Undoped materials are anti-ferromagnetic Mott insulators

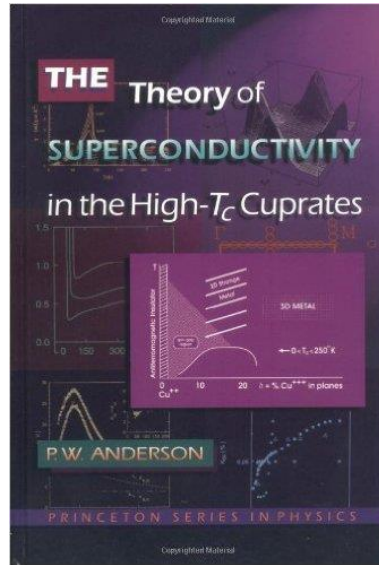
Doping → competition S.C. and antiferromagnetism
spin fluctuations are important (glue??)

d-wave superconductors

Formula	Notation	T _c (K)	#Cu-O planes	Crystal structure
Bi ₂ Sr ₂ Ca ₂ Cu ₃ O ₆	Bi-2223	110	3	Tetragonal
Bi ₂ Sr ₂ CaCu ₂ O ₈	Bi-2212	85	2	Tetragonal
Bi ₂ Sr ₂ CuO ₆	Bi-2201	20	1	Tetragonal
HgBa ₂ Ca ₂ Cu ₃ O ₈	Hg-1223	134	3	Tetragonal
HgBa ₂ CaCu ₂ O ₆	Hg-1212	128	2	Tetragonal
HgBa ₂ CuO ₄	Hg-1201	94	1	Tetragonal
Tl ₂ Ba ₂ Ca ₂ Cu ₃ O ₁₀	Tl-2223	125	3	Tetragonal
Tl ₂ Ba ₂ CaCu ₂ O ₈	Tl-2212	108	2	Tetragonal
Tl ₂ Ba ₂ CuO ₆	Tl-2201	80	1	Tetragonal
TlBa ₂ Ca ₃ Cu ₄ O ₁₁	Tl-1234	122	4	Tetragonal
YBa ₂ Cu ₃ O ₇	123	92	2	Orthorhombic

wikipedia

conductivity and superconductivity. On this basis I was able to explain most of the experimental data about layered cuprates without dividing them into “good” ones, which should be mentioned on every possible occasion, and “bad” ones, which should be forgotten. As a result I can state that the so called “mystery” of high- T_c superconductivity does not exist.



Abrikosov, NP 2003

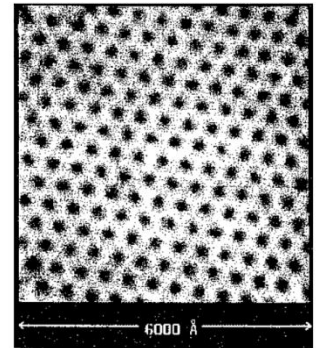
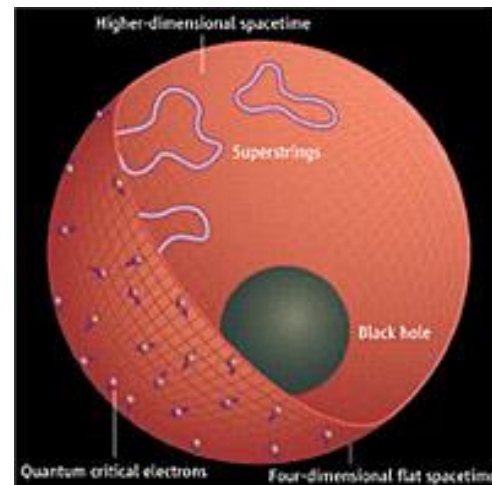


Figure 6. Vortices in NbSe₂ defined by scanning tunneling microscopy (STM)

Theory of High- T_c Superconductivity: Transition Temperature

Dale R. Harshman^{1,2,3,6}, Anthony T. Fiory⁴ and John D. Dow^{3,5}



ADS/CFT theories for HTc's (image: P. Huey, Science 2008)

Sr_2RuO_4

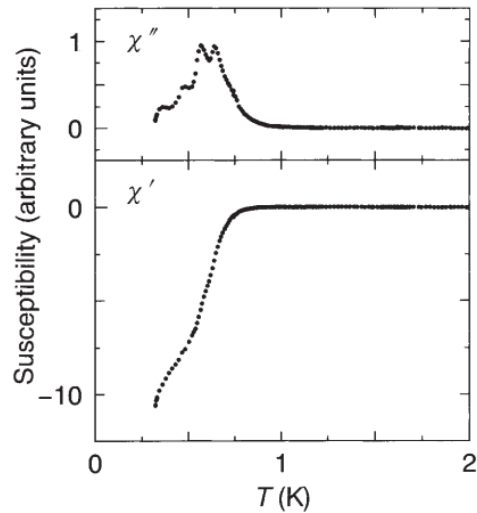


FIG. 2 The a.c. susceptibility of a single crystal of Sr_2RuO_4 measured by a mutual-inductance method at a magnetic field of $H = 0.67$ Oe (root-mean-squares value) parallel to the c -axis, and at a frequency of 1,000 Hz. Top, χ'' (imaginary part); bottom, χ' (real part).

Maeno et al., Nature 1994

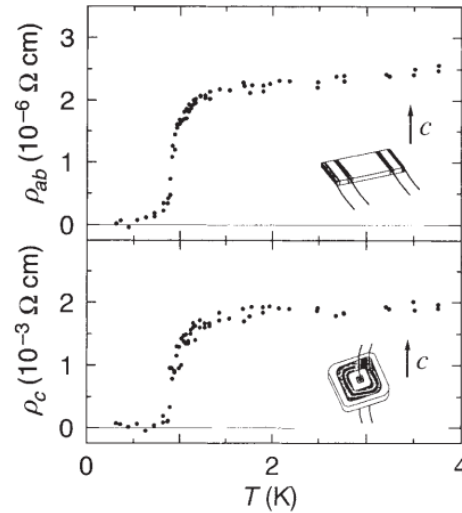
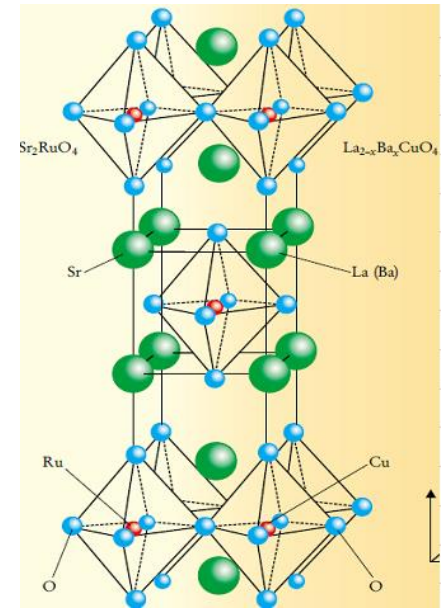


FIG. 3 Anisotropy in the resistivity ρ of Sr_2RuO_4 below 4 K. The superconducting transition is at $T_c = 0.93$ K. Insets, attachment of the electrodes.



$T_c = 1.5$ K

p-wave superconductor

For review see e.g. Maeno, Rice, Sigrist, Phys. Today, Jan. 2001

LETTERS

Superconductivity at 43 K in an iron-based layered compound $\text{LaO}_{1-x}\text{F}_x\text{FeAs}$

Hiroki Takahashi¹, Kazumi Igawa¹, Kazunobu Arii¹, Yoichi Kamihara², Masahiro Hirano^{2,3} & Hideo Hosono^{2,3}

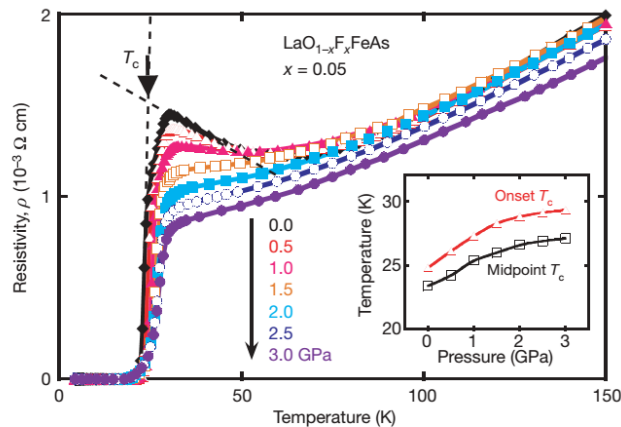


Figure 3 | Temperature dependence of the electrical resistivity of $\text{LaO}_{0.95}\text{F}_{0.05}\text{FeAs}$ below 3 GPa, using the piston–cylinder device. The inset shows the pressure dependence of the onset and midpoint T_c s. The onset T_c increases with increasing pressure, with an initial slope of 2.0 K per GPa.

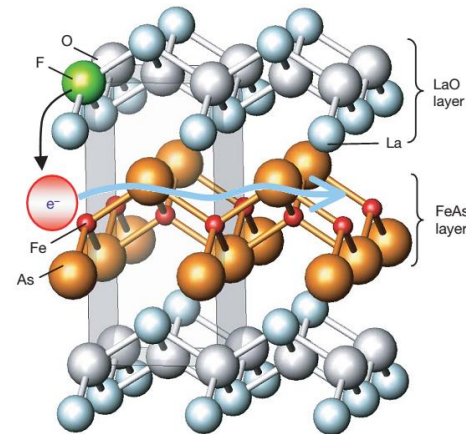
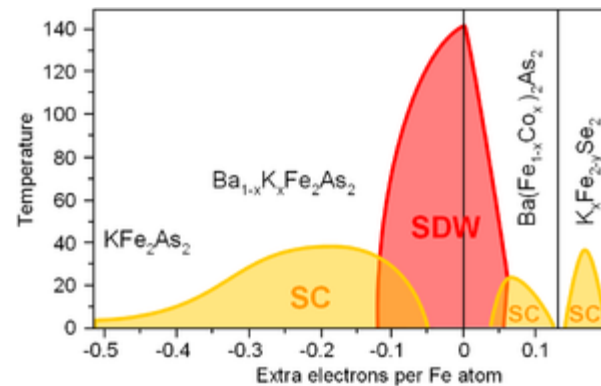


Figure 1 | Schematic crystal structure of LaOFeAs . Electron carriers



Heterostructure oxide interfaces

$T_c \sim 200$ mK

Heterostructure of wide bandgap materials

LaAlO₃: 5.6 eV; SrTiO₃ 3.2 eV

2D electron gas at interface

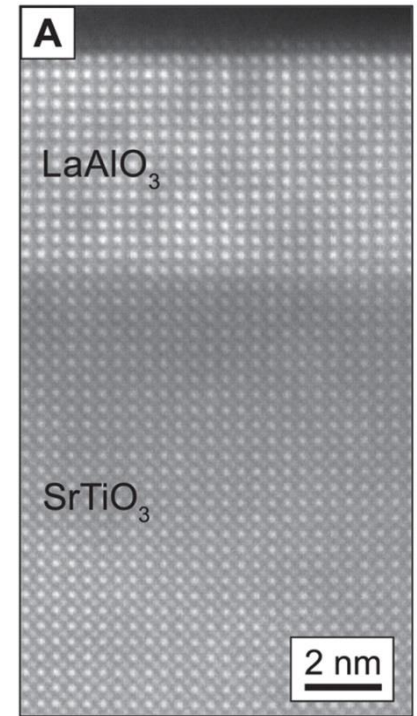
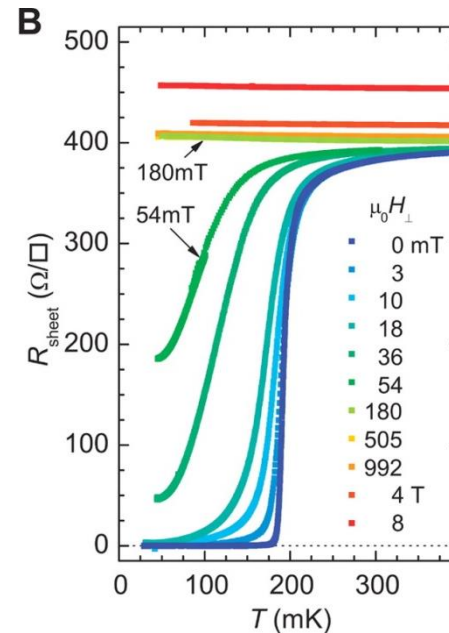
- Oxygen stoichiometry?
- Polar catastrophe?

SrTiO₃: Stack of neutral layers (SrO/TiO₂/...)

LaAlO₃: Charged layers (LaO⁺/AlO₂⁻/...)

LaAlO₃ Polar surface? : leads to divergent potential

→ electronic reconstruction



Reyren et al., Science 317, 1196 (2007)

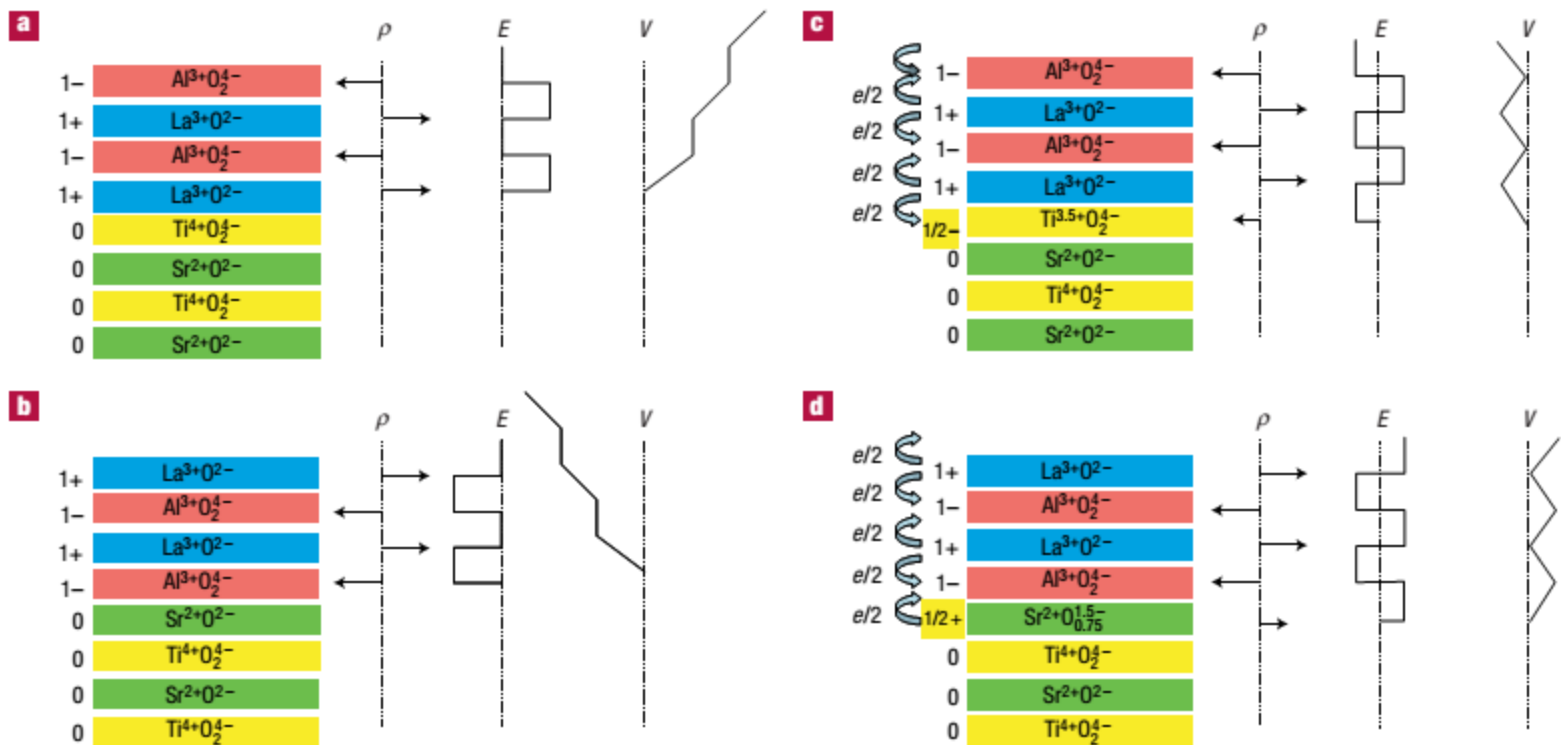


Figure 1 The polar catastrophe illustrated for atomically abrupt (001) interfaces between LaAlO_3 and SrTiO_3 . **a**, The unreconstructed interface has neutral (001) planes in SrTiO_3 , but the (001) planes in LaAlO_3 have alternating net charges (ρ). If the interface plane is $\text{AlO}_2/\text{LaO}/\text{TiO}_2$, this produces a non-negative electric field (E), leading in turn to an electric potential (V) that diverges with thickness. **b**, If the interface is instead placed at the $\text{AlO}_2/\text{SrO}/\text{TiO}_2$ plane, the potential diverges negatively. **c**, The divergence catastrophe at the $\text{AlO}_2/\text{LaO}/\text{TiO}_2$ interface can be avoided if half an electron is added to the last Ti layer. This produces an interface dipole that causes the electric field to oscillate about 0 and the potential remains finite. The upper free surface is not shown, but in this simple model the uppermost AlO_2 layer would be missing half an electron, which would bring the electric field and potential back to zero at the upper surface. The actual surface reconstruction is more complicated²¹. **d**, The divergence for the $\text{AlO}_2/\text{SrO}/\text{TiO}_2$ interface can also be avoided by removing half an electron from the SrO plane in the form of oxygen vacancies.

Superconducting materials

- Many, many superconducting materials
- High debye frequency (conventional SC)
- High DOS at fermi level
- Low dimensionality favorable
- Competing interactions, vicinity other phase transitions
- On-site coulomb suppresses s-wave
- Electronic mechanisms (charge, spin)
- No theoretical limit for T_c (at this point in time)

